Mater. Res. Soc. Symp. Proc. Vol. 1165 © 2009 Materials Research Society 1165-M09-01

Magnetron sputtering for II-VI solar cells: thinning the CdTe

V. V. Plotnikov, A. C. Vasko, A. D. Compaan, X. Liu, K. A. Wieland, R. M. Zeller, J. Li, R. W. Collins

Department of Physics and Astronomy, and Wright Center for Photovoltaics Innovation and Commercialization, The University of Toledo, Toledo, OH 43606

ABSTRACT

Magnetron sputtering (MS) of CdTe and related II-VI materials facilitates low energy ion and electron bombardment that promotes good film growth at substrate temperatures well below those needed for other physical vapor deposition methods. MS also provides good control of deposition rates while allowing scale-up to large areas. In this paper we review the use of MS for deposition of polycrystalline thin films of CdS, CdTe and related materials for solar cells with a focus on reducing the thickness. We relate the deposition conditions and plasma properties determined by Langmuir probe measurements to some of the materials properties of the films through spectroscopic ellipsometry and high resolution electron microscopy. For cells with CdTe layers from 0.35 to 2.5 μm, we have done a first-order optimization of chloride treatment conditions and back contact structure. We discuss the influence of CdTe thickness and post-deposition processing on the efficiency, open-circuit voltage, short-circuit current, and fill factor and show that 10% efficient cells can be fabricated with 0.5 μm of CdTe.

INTRODUCTION

Reduction of absorber layer thickness in thin-film solar cells can speed the fabrication process, which is particularly important for lower-speed deposition methods, reduce the demand for source or feedstock materials, extend supplies and thereby enlarge the ultimate market penetration, lessen environmental concerns, and facilitate recovery of materials at the end of life. In addition, the use of extremely thin layers, while maintaining efficiency, can open new applications such as semitransparent photovoltaic coatings for architectural glazing.

In this paper we describe our studies with sputter deposition for achieving the high quality absorber layers that can facilitate fabrication of cells with CdTe thickness well below one micron. Understanding the plasma conditions through the use of a Langmuir probe, *in situ* monitoring of the deposition process with spectroscopic ellipsometry and optical reflection, as well as optimization of the post-deposition treatments have been keys to the achievement of an efficient cell with less than 0.5 μm of CdTe.

EXPERIMENTAL DETAILS

We have shown that rf sputtering of ZnO:Al, CdS, and CdTe layers can produce 14% efficient cells on 1 mm aluminosilicate glass (ASG).[1] In addition, we have shown that ~12.5% efficient cells can be prepared by sputtering on commercially available 3 mm coated soda lime glass (Pilkington TEC-15).[2, 3] In recent work we have exceeded 13% cells on TEC-15 if a high

resistivity transparent (HRT) layer is used between the SnO_2:F and the CdS layer. In the case of ASG substrates, we have not yet used an HRT layer which facilitates the use of thinner CdS and yields higher current. In the case of TEC-15 substrates with the HRT layer, the current is limited by some absorption in the glass and in the commercial SnO_2:F which was developed for low-emissivity (low-E) archictectural glass. Thus we expect that rf sputtering can yield best cell efficiencies that are within about one percent absolute of the champion CdTe cells on these materials.[4]

IN SITU STUDIES OF THE DEPOSITION PROCESS

Earlier work has shown that an unbalanced magnetic field magnetron has advantages in yielding higher performance cells probably due to the greater flux of Ar ions and electrons on the film growth interface.[5] The NdFeB magnet geometry and the B-field configuration[6] are sketched in Fig. 1. Low energy ion bombardment of the growing film is sensitive not only to the magnetic field configuration but also to the sputter gas pressure, target-substrate separation, and the location of grounded surfaces. A Langmiur probe (See Fig. 2.) was used to measure the DC plasma potential and thus the target sheath potential and the substrate sheath potential. This allows estimates of the energy of ions impacting the growth interface. The target potential was measured directly via the powered electrode after the impedance matching network. The substrate holder was insulated from the chamber ground and was allowed to reach an equilibrium floating potential. The measurements are summarized in Fig. 3 and show clearly that the potentials vary with the rf power and with the proximity of grounded surfaces. We show two extreme cases—for a freshly cleaned (acid etched) ground shroud and for a ground shroud that has accumulated a thick insulating coating after several depositions of CdTe.

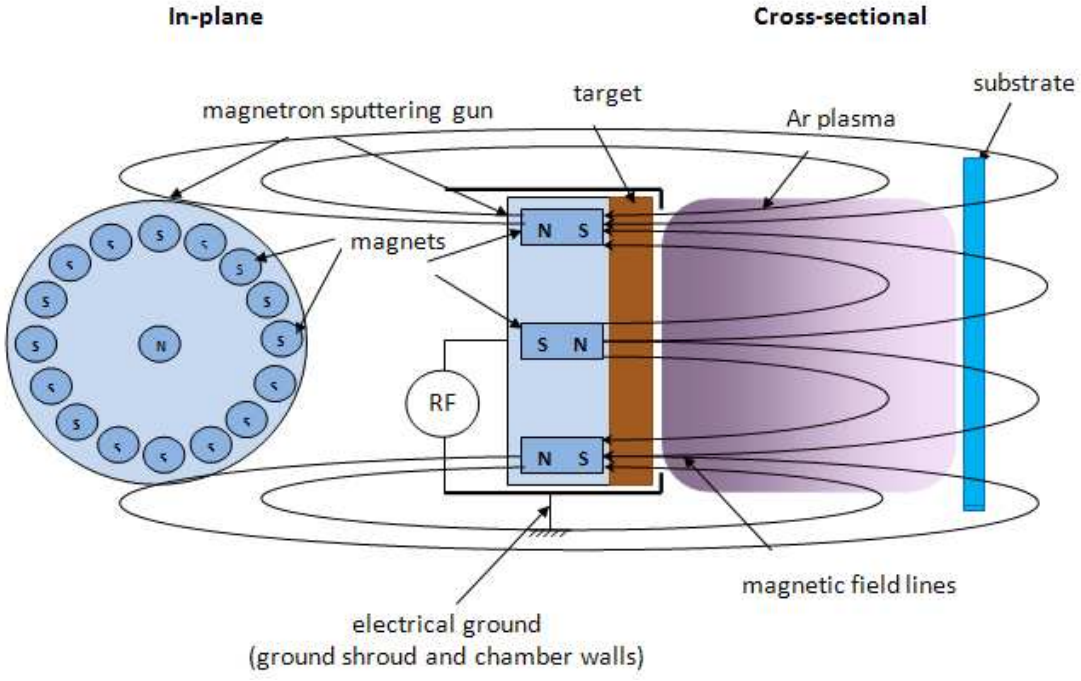

Fig. 1. In-plane and cross-sectional views of the balanced (top) and unbalanced (bottom) magnetron sputtering system.

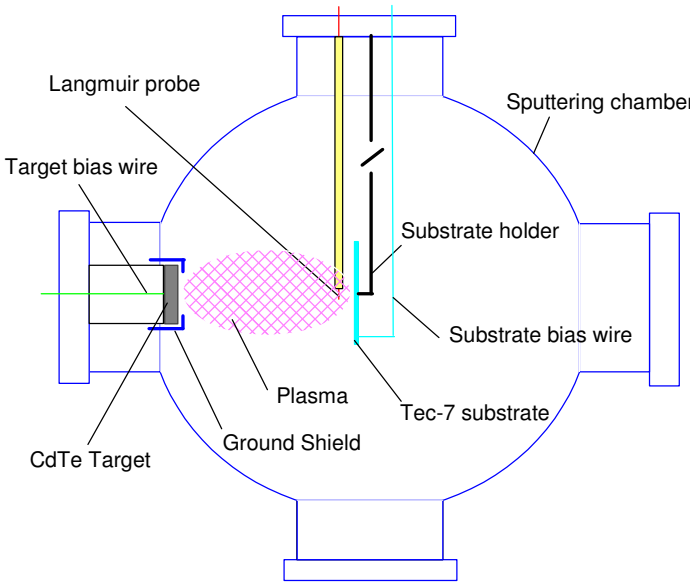

Fig. 2. Experimental setup for potential distribution measurements via a Langmuir probe.

Fig. 3b shows that the plasma potential is lower by 5 – 8 volts when the sputter gun ground shroud is freshly cleaned. That is, when the closest grounded surface becomes insulating, the plasma potential rises by a few volts. Correspondingly however, the target DC self-bias also rises slightly and the self bias potential of the substrate also rises by 5-10 volts. Thus there is little change in either the target sheath potential, which determines the sputter ion energies and thus the sputtering rate, or the substrate sheath potential, which determines the low energy ion energy impacting the growing film.

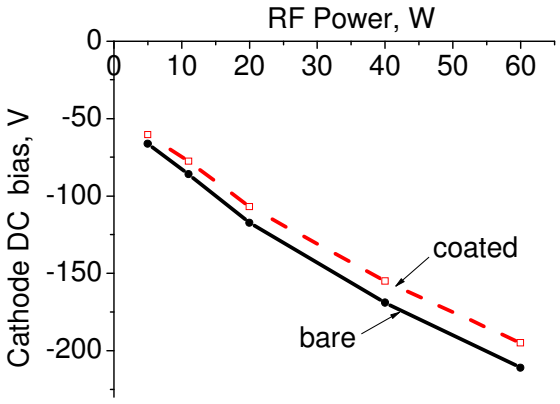

Fig. 3a. Target cathode DC bias as a function of pressure and RF power. Bare ground shroud (solid lines) and coated ground shroud (dashed lines).

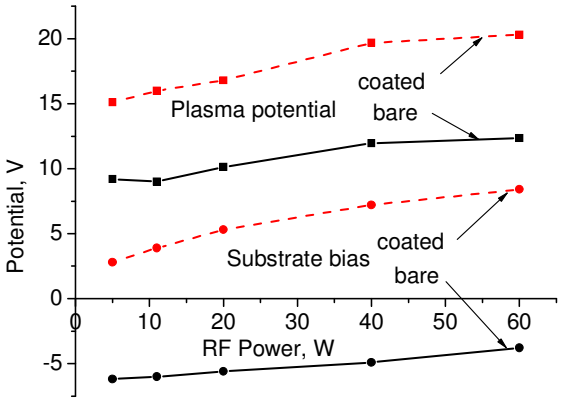

Fig. 3b. Plasma potential (upper) and substrate self-bias bias as a function of pressure and RF power. Bare ground shroud (solid lines) and coated ground shroud (dashed lines)

For the preparation of cells with very thin absorber layers, it is essential to have accurate real-time monitoring of the growth. This has been done in two ways. We have used a 980 nm diode laser in reflection from the substrate and the growing films. Fig. 4 illustrates typical data. The deposition system uses two sputter sources (CdS and CdTe) angled at about 20 degrees to the normal to the rotating substrate which is facing downward. The incident and reflected laser beams are also at about 40 degrees through windows in the chamber between the sputter sources.

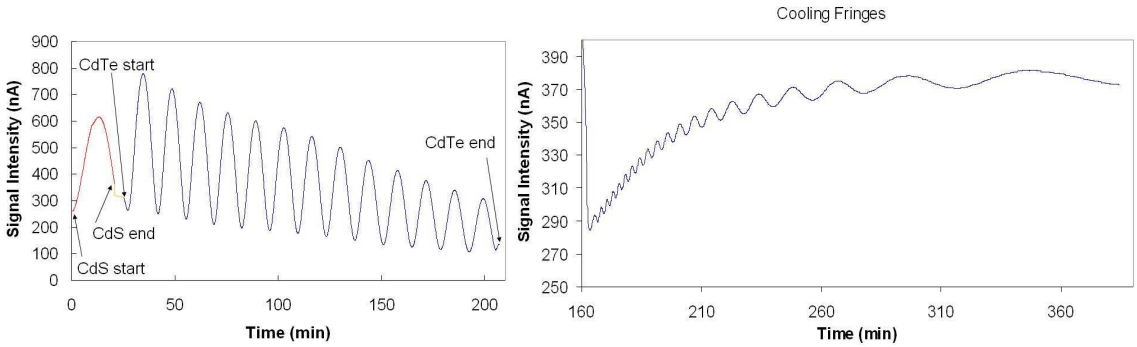

Fig. 4. Interference fringes from reflection monitor at 980 nm. CdS growth is followed by CdTe growth and separately on a longer timescale, fringes arise from the TEC-15 glass underneath the CdS/CdTe as the substrate cools from ~270 ^{o}C to room temperature.

Much more detailed in-situ characterization has been done using real-time spectroscopic ellipsometry (RTSE).[7] Details of this RTSE system for studying CdTe growth have been given in Ref. 6. Some data especially relevant to the preparation of very thin films of CdTe are shown in Fig. 5 which shows surface roughness, d_s, as a function of the bulk layer thickness, d_b, of the film. The nucleation stage (left) shows a monotonic change from the Volmer-Weber (V-W) island growth mode at lower T_d to the Stranski-Krastanov (S-K) layer-island growth mode at higher T_d. The longer term d_s evolution (right, when $d_b > 2000$ Å) shows a monotonic trend of surface smoothening at higher T_d. Both trends are consistent with enhanced surface diffusion at higher T_d. Note that surface roughness is lowest in the range of 250 to 300 ^{o}C for films of ~3000 Å or 0.3 μm.

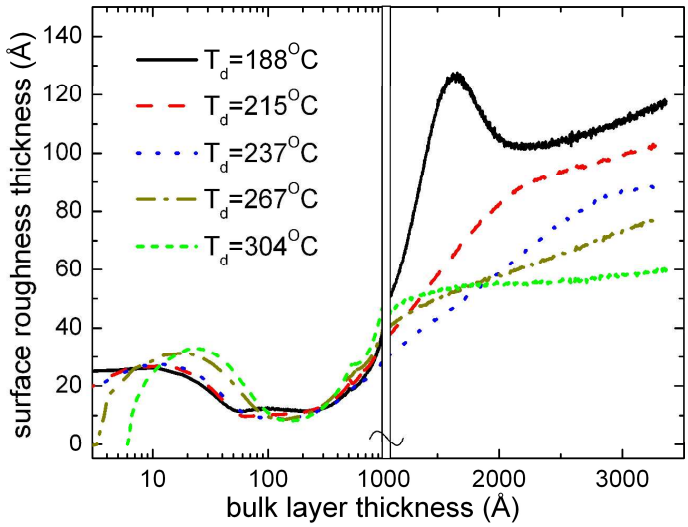

Fig. 5. Surface roughness thickness (d_s) evolution with bulk film thickness (d_b) for CdTe films magnetron sputtered on c-Si wafer substrates held at different temperatures (T_d) but with otherwise identical deposition parameters (rf power of 60 W and Ar pressure of 18 mTorr).

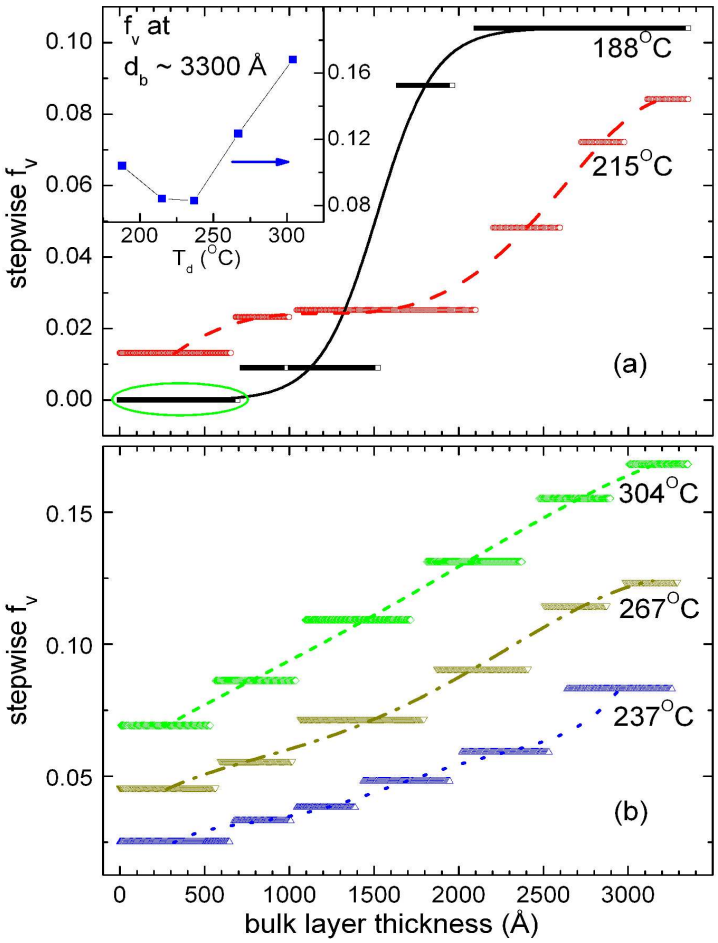

Fig. 6. Stepwise evolution of void volume fraction (f_v) for the CdTe films of Fig. 5 magnetron sputtered on c-Si wafer substrates held at different T_d.

The RTSE data also provide information on the bulk material under the surface roughness layer. This is obtained from a step-wise analysis of the SE data in which each step builds self-consistently on the underlying, previously deposited, layer. This modeling of the data shows that for all deposition temperatures, T_d, the bulk void fraction, f_v, increases monotonically with increasing bulk layer thickness. In the thin-film regime ($d_b < 500$ Å), f_v increases monotonically with increasing T_d. The lowest T_d film, 188 °C, has the lowest f_v value in the initial stages; however, it exhibits an abrupt structural transition at $d_b \sim 1500$ Å where f_v increases by more than eight times within a narrow d_b range. This transition is attributed to strain relaxation and the effect is suppressed with increasing T_d, as the initial void fraction increases. f_v in the top-most layer of the final film is shown as a function of T_d in the inset. The highest density in the near-surface region of the final film (~ 3300 Å) is obtained near $T_d \sim 230$°C. This is marginally below the deposition temperature that had earlier been chosen for most of the cell fabrication work. It is reasonable that both surface roughness and voids provide means for strain relaxation in the films.

HIGH RESOLUTION CROSS-SECTIONAL STUDIES OF CdS/CdTe CELLS

One of the major concerns with very thin absorber layers is that atomic species from the back contact may diffuse to the junction and degrade the quality of the active CdS/CdTe junction. Of particular concern is copper which is almost universally used in the back contact. For our sputtered films, no chemical etching of the CdTe surface was used in preparation for the evaporated 3nm Cu/ 20 nm Au back contact. We anticipate that grain boundaries may serve as a fast diffusion channel for the Cu. To study this we prepared cells with our standard 2.3 μm CdTe thickness and our standard vapor $CdCl_2$ and back contact processes. Cross sectional samples were prepared and thinned to electron transparency for TEM studies and small spot energy dispersive x-ray spectroscopy (EDS). Fig. 7 shows the TEM image with two grain boundaries highlighted with dashed lines. Several small circles indicate the locations at which EDS spectra were obtained. The circle size indicates the estimated size of the area of x-ray fluorescence and the numbers next to the circles indicate the ratio of the Cu k_α x-ray intensity to a fluorescence peak from the Mo mounting ring, which was used as a convenient normalizing reference. These ratios are shown in Table 1. Exactly at the Cu/Au interface (eds-a) the Cu/Mo ratio is 2.24 and the two circles in the Au layer (eds-b, c) with ratios of 1.73 and 1.61 show that Cu has diffused into the Au layer to form a Cu/Au alloy. But three ratios from spots along a grain boundary in CdTe (eds-e, d, f have ratios of 0.32, 0.27 and 0) with Cu k_α x-ray intensities that are near the detection limit. Although the Cu EDS signal does not yield trace level detection, these data do indicate that Cu diffusion along grain boundaries is very low as near as 50 nm from the back contact. We think that the good results on the very thin cells, shown below, confirm that Cu diffusion is not a serious problem for absorber thicknesses well below 1 μm.

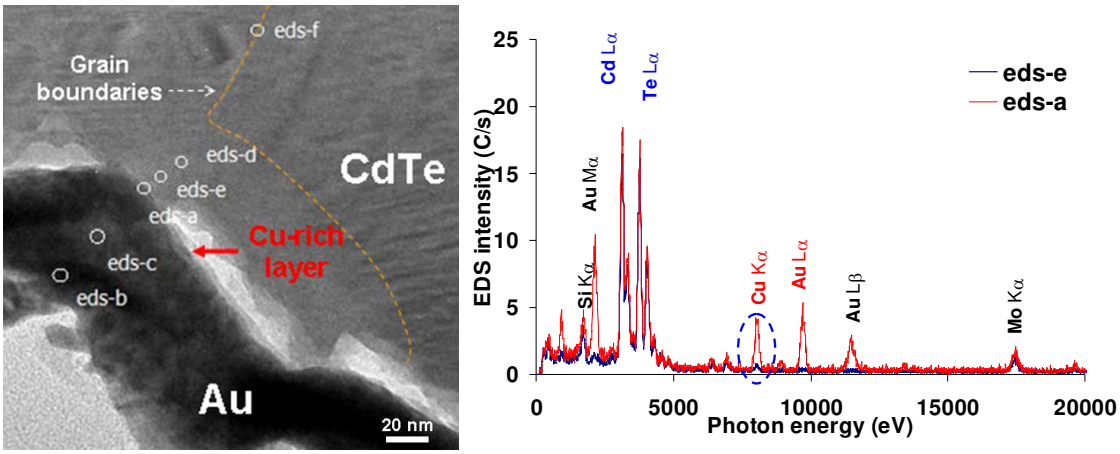

Fig. 7. a) Cross-section TEM image of CdTe and Au layer. Circles are the locations where the fine-probe EDS spectra were taken. Broken line indicates the grain boundary of CdTe. b) EDS spectra from CdTe/Au interface (eds-a) and shallow CdTe surface (eds-e).

Table 1. Comparison of Cu/Mo intensity ratios.

Position	Cu/Mo peak intensity ratio
eds-b	1.61
eds-c	1.73
eds-a	**2.24**
eds-e	0.32
eds-d	0.27
eds-f	0

CELL PERFORMANCE vs. CdTe THICKNESS

The cells for this thickness dependence study were prepared on TEC-15 glass with an HRT coating. For reproducibility, we chose to use a CdS layer thickness of 60 nm, slightly greater than the 30-50 nm that we have identified as giving optimum efficiency for these substrates. (Thinner CdS yields higher cell current (J_{SC}) but if the CdS is too thin, V_{OC} and FF decrease rapidly even for 2 μm of CdTe.) Choosing the CdS thickness slightly greater than optimum helps to assure strong electrical properties on the n-side of the junction. Thus the variations in cell performance should be due mainly to the properties of the CdTe and the back contact side of the device.

We prepared a set of samples with the following CdTe thicknesses: 0.38 μm, 0.5 μm, 0.65 μm, 0.8 μm, 1.1 μm, 1.45 μm, 1.85 μm, 2.2 μm and 2.6 μm. Thickness was measured by a DEKTAK profilometer. For each CdTe thickness we used four different combinations of two different $CdCl_2$ treatments and two different back-contact recipes. We used $CdCl_2$ treatment times of 38 minutes and 5 minutes while keeping the temperature constant at 387 ^oC. Treatment was done in a tube furnace flushed with dry air. The contribution of the heat-up and cool-down time was also estimated and taken into account. The back contact structure was our standard, thermally activated Cu/Au bilayer deposited by thermal evaporation. The Au thickness was 20 nm and the thickness of the Cu layer was chosen to be either 30 Å or 10 Å. The Cu activation time ranged from 45 minutes to 5 minutes at 150 ^oC in ambient air.

Each sample, representing a unique combination of CdTe thickness/$CdCl_2$ treatment time/back contact scheme contained 35 dot cells of 0.062 cm^2 area. Cells were tested by J-V and apparent quantum efficiency (AQE). The J-V characteristics of one of the best cells for each CdTe thickness are shown in Fig. 8. Note that the V_{OC} is above 750 mV for cells with 0.65 μm or more of CdTe; however, the J_{SC} and FF decrease below 1 μm.

We found a very little decrease of the overall cell efficiency for thicknesses down to 1 micron as long as the post-deposition conditions were close to the optimum. This can be seen from Fig. 9 where the best cell efficiency is plotted against the CdTe thickness. Overall we found that for cells of 0.85 μm and above, variations in the thickness of as-deposited Cu and in the Cu diffusion time make a greater difference than variations in the duration of the $CdCl_2$ treatment. For instance using 30 Å of as-deposited Cu instead of 10 Å led to an increase of the average V_{OC} by much as 50 mV for 1.85 μm of CdTe and this trend was consistent throughout the whole range of thicknesses (0.85μm to 2.6 μm). A similar dependence was observed in the fill factor as well, namely that thinner cells optimized with thinner Cu layers and shorter diffusion times.

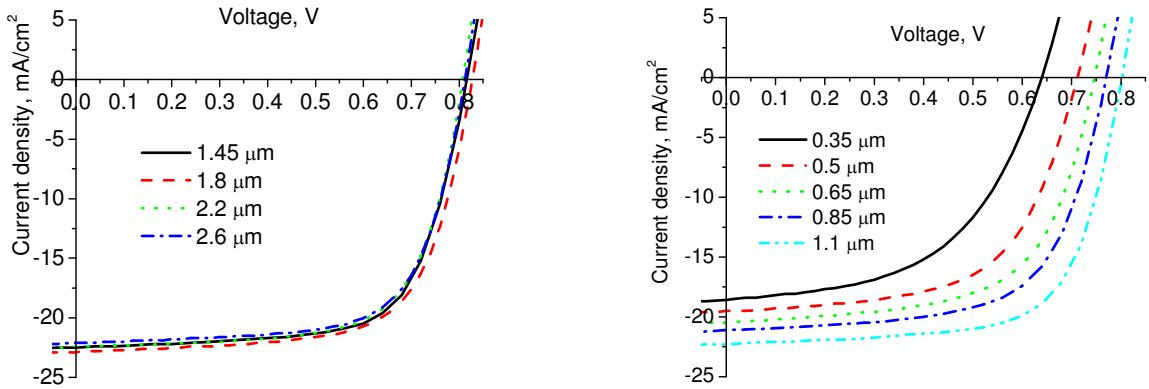

Fig. 8. J-V characteristics of the cells with different CdTe thicknesses.

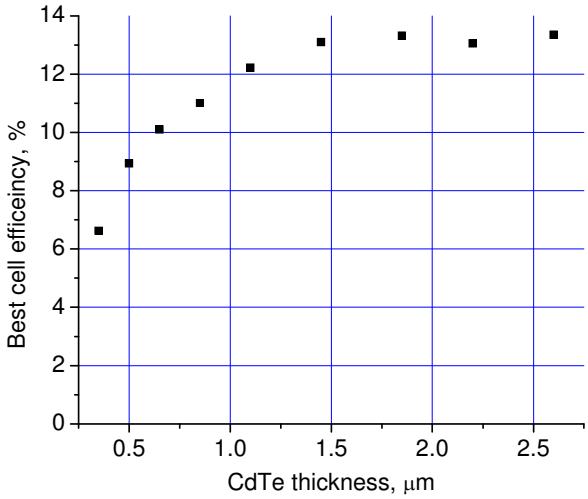

Fig. 9. Best cell efficiency as a function of CdTe thickness

The situation gets more complicated for the thinner samples (below 0.85 μm). We have not seen a clear dependence on either $CdCl_2$ treatment duration or back contact scheme, yet certain guidelines were established. Overall we have fabricated cells with efficiency above 12% for the CdTe thickness of 1 μm and above 9 % for the 0.5 μm CdTe. Typically the thinnest cells optimize with 10 to 20 Å of Cu diffused for 5 minutes and have a chloride treatment time of 5 minutes at 387 C.

The AQE reveals stronger voltage-dependent collection for the thinner cells. (Results for the 1.1 μm and 0.65 μm CdTe cells are shown for comparison in Fig. 10). Our calculations also show that the collection efficiency from the space-charge region is less than unity for these cells even under the reverse bias conditions which is suggestive of some unidentified recombination mechanism that is absent in the thicker cells. These effects are under investigation through temperature-dependent J-V studies.

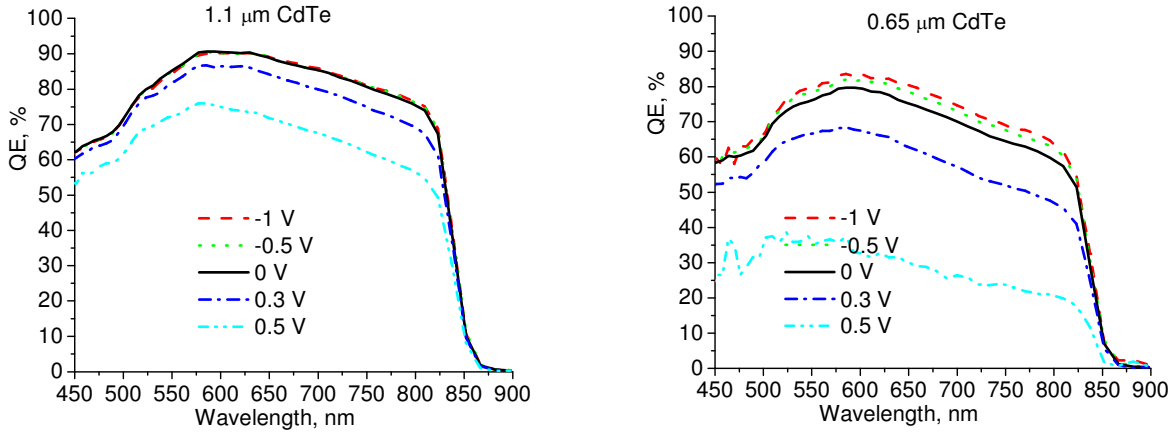

Fig. 10. Voltage dependence of external apparent quantum efficiency of cells with 1.1 μm and 0.65 μm of CdTe.

CONCLUSIONS

We investigated the dependence of the cell performance over a wide range of CdTe thicknesses from 0.35μm to 2.6μm. We find that that an average efficiency of greater than 12% can be achieved for cells as thin as 1 micron with the appropriate post-deposition treatment and optimized back contact scheme. For CdTe thicknesses of one micron and above, we find the effect of the back contact scheme (as-deposited Cu thickness) to be more dramatic than variation in $CdCl_2$ treatment time. Insufficient Cu caused an average V_{OC} reduction of as much as 50 mV in some cases, while the use of adequate amounts of Cu yielded V_{OC} of 800 mV or above for all samples above 1 μm.

We also found that reduction of CdTe thickness below 1 μm leads to a gradual decrease in performance although 10% efficiency can be obtained with 0.5 micron CdTe. Much of the efficiency loss is due to incomplete photoabsorption. In fact modeling the J_{SC} according to single-pass absorption with no optical reflection at the back contact accounted for most of the current loss in the best of the thin cells. More studies are underway to resolve the issues of the V_{OC} and FF losses as well as collection probability less than unity from the space charge region in the thin cells. In addition, modeling of appropriate optical reflector structures is underway.

ACKNOWLEDGMENTS

This work was supported by the NREL Thin Film Partnership program, the DOE-SAI University Photovoltaic Process and Product Development program, and the Ohio Department of Development. The collaboration of Dr. Kai Sun for the TEM and EDS studies is greatly appreciated.

REFERENCES

[1] A. Gupta and A.D. Compaan, "All-sputtered 14% CdS/CdTe thin-film solar cell with ZnO:Al transparent conducting oxide," Appl. Phys. Ltrs., **84**, 684 (2004).

[2] M. Shao, A. Fischer, D. Grecu, U. Jayamaha, E. Bykov, G. Contreras-Puente, R.G. Bohn, and A.D. Compaan, "Radio-frequency-magnetron-sputtered CdS/CdTe solar cells on soda-lime glass," Appl. Phys. Lett. 69, 3045-3047 (1996).

[3] A.D. Compaan, "Photovoltaics: clean power for the 21st century" Solar Energy Materials & Solar Cells, **90**, 2170-2180 (2006)

[4] X. Wu, J.C. Keane, R.G. Dhere, C. DeHart, D.S. Albin, A. Duda, T.A. Gessert, S. Asher, D.H. Levi, P. Sheldon, "16.5%-Efficient CdS/CdTe Polycrystalline Thin-Film Solar Cell." McNelis, B., et al., eds. Seventeenth European Photovoltaic Solar Energy Conference: Proceedings, pp. 995-1000 (2002).

5 R. Wendt, A. Fischer, D. Grecu and A.D. Compaan, "Improvement of CdTe solar cell performance with discharge control during film deposition by magnetron sputtering," J. Appl. Phys. 84, 2920-2925 (1998).

6 A.D. Compaan, M. Shao, A. Fischer, D. Grecu, U. Jayamaha, G. Conteras-Puente, and R.G. Bohn, "Effects of Magnetic Field Configuration on RF Sputtering for CdS/CdTe Solar Cells," Materials Research Society Symp. Proc. 426, 391-96 (1997).

7 Jian Li, Jie Chen, N.J. Podraza, and R.W. Collins, "Real Time Spectroscopic Ellipsometry of Sputtered CdTe: Effect of Growth Temperature on Structural and Optical Properties", Conference Record of the IEEE 4th World Conference on Photovoltaic Energy Conversion 2006, (IEEE, Piscataway NJ, 2006) pp. 392-395.